Lawrence Berkeley National Laboratory
LBL Publications

Title

Triptycene-Based Molecular Rods for Langmuir-Blodgett Monolayers

Permalink
https://escholarship.org/uc/item/3tt4x8w5

Journal
ChemPlusChem, 87(4)

ISSN
0010-0765

Authors
Kaletová, Eva
Hurtado, Carina Santos
Císařová, Ivana
et al.

Publication Date
2022-04-01

DOI
10.1002/cplu.202200023

Copyright Information
This work is made available under the terms of a Creative Commons Attribution-NonCommercial License, available at https://creativecommons.org/licenses/by-nc/4.0/

Peer reviewed

eScholarship.org Powered by the California Digital Library
University of California

Triptycene-Based Molecular Rods for Langmuir-Blodgett Monolayers

Eva Kaletová,[a] Carina Santos Hurtado,[a] Ivana Císařová,[b] Simon J. Teat,[c] and Jiří Kaleta[a]*

[a] *Institute of Organic Chemistry and Biochemistry of the CAS, Flemingovo nám. 2, 160 00 Prague 6, Czech Republic.*
[b] *Department of Inorganic Chemistry, Faculty of Science, Charles University in Prague, Hlavova 2030, 12840 Prague 2, Czech Republic.*
[c] *Advanced Light Source, Lawrence Berkeley National Laboratory, 1 Cyclotron Road, Berkeley, CA 94720, U.S.A.*

TOC Graphic

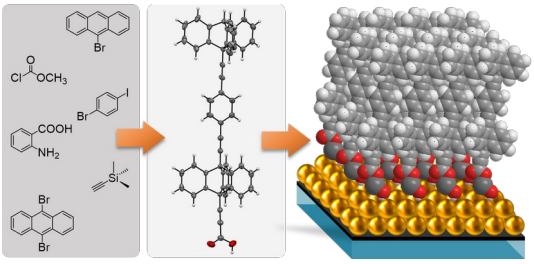

ABSTRACT

Herein we introduce fully modular synthesis leading to three representative examples of rigid molecular rods that are intended to form sturdy self-assembled monolayers (SAMs) on various surfaces. These molecules contain two triptycene units that are designed to interlock into a compact "double-decker" structure. Two of the three final products provided suitable crystals for X-ray diffraction, allowing deeper insight into packing in the 3-D crystal lattice. The acidity of all three compounds were determined by capillary electrophoresis, and the pK_a values ranged between 2.06-2.53. All three rigid rods easily formed SAMs on the water-air interfaces, with the area per molecule equal to 55-59 Å^2/molecule, suggesting tight intermolecular packing. The thickness of all three SAMs reached ~19 Å after transfer to a gold (111) surface, meaning that individual molecules are tilted maximally 38° from the axis perpendicular to the surface. These geometrically unique molecules represent promising platforms with a wide scope of applicability in the supramolecular architecture.

INTRODUCTION

Molecular machines involving various molecular rotors, motors and switches are widely studied systems with a potentially broad scope of applicability (for example smart materials, memory devices, artificial molecular "muscles", etc.).[1,2,3,4,5,6] They have been thoroughly investigated not only (i) in solution and (ii) in solid-state as ordered 3-D materials,[7,8,9,10] but also on (iii) interfaces (solid-liquid, solid-gas, liquid-gas), mostly in the form of regular 2-D arrays.Error: Reference source not found[,11,12,13,14,15,16,17,18] In particular, using interfaces is highly attractive as it combines the ability of molecular machines to freely operate, which is characteristic for systems in solution, with a high order typical for crystalline materials. There are several strategies used to facilitate sufficient separation between neighboring molecules: probably the most widely used is based on the utilization of various platforms/stands that anchor individual molecules to the surface while still providing sufficient separation from neighbors.Error: Reference source not found[,Error: Reference source not found,Error: Reference source not found,Error: Reference source not found,19]

We are particularly interested in triptycene-based stands, since these versatile systems are easily available in multigram quantities, are highly robust, allow numerous chemical modifications, and can be easily adjusted to various surfaces.Error: Reference source not found[,Error: Reference source not found,Error: Reference source not found,Error: Reference source not found,20]

Herein we introduce three molecular rods **1**-**3**, that are designed to form self-assembled monolayers (SAMs) on a water-air interface using the Langmuir-Blodgett technique (Chart 1). Subsequently, they can be transferred to various solid substrates. These rod-shaped amphiphilic systems share two characteristic units (carboxylic function and two triptycene cages), and differ in the nature of the aromatic cores placed in the middle of the rods. The carboxylic functions that are located on one rod terminus facilitate interaction with the aqueous subphase during the monolayer formation. The triptycene cores are intended to interlock into a double-decker system via interactions with neighboring molecules. This will result in a sandwich-like structure accommodating (hetero)aromatic rings in between these two "layers". The intermolecular separation is dictated by the length of the triptycene paddle (~5.2 Å). On top of that, compounds **2** and **3** can serve as molecular rotors since they carry difluorophenyl and pyridazinyl cores, both with high dipole moments (2.5 D for 1,2-difuorobenzene[21] and 4.1 D for pyridazine[22] itself). The whole concept can be expanded even more, and the next generation of these rod-like structures can carry various molecular machines on the top of the upper triptycene unit (attached to the bridgehead position). Since our motivation is the desire to improve our understanding of the effect of molecular flexibility on packing within SAMs, we designed **1**-**3** as shorter and thus stiffer alternatives to the already knownError: Reference source not found **4** and **5**. The presence of butadiyne linkers in these two previously reported structures facilitates synthetic operations, but also introduces undesired flexibility into the system. Detailed structural investigation of all these films will be published separately.

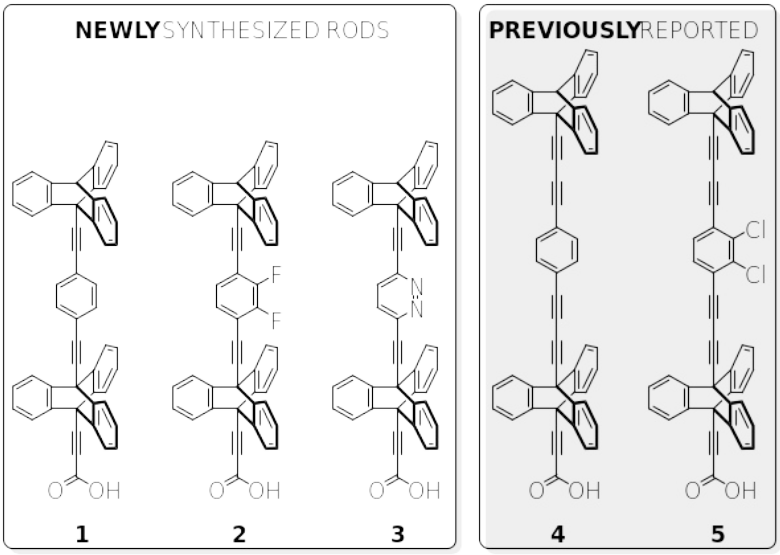

Chart 1. Structures of newly synthesized molecular rods **1**-**3** and structurally related previously reportedError: Reference source not found systems **4** and **5**.

RESULTS AND DISCUSSION

Here we report the synthesis of three rigid molecular rods **1**-**3**, crystallographic data for five compounds including **1** and **2**, and acidity constants for **1**-**5**. We are also providing a

basic characterization of corresponding SAMs, including the Langmuir-Blodgett isotherms for **1**-**3**.

Synthesis. A fully modular approach based on using two crucial triptycene-based building blocks **6Error: Reference source not found** and **7Error: Reference source not found** was utilized to construct the complex rigid rods **1**-**3**. The synthesis started with Sonogashira coupling between alkyne **6** and (hetero)aryl iodides **8**-**10**, which resulted in the formation of the expected products **11**-**13**, from moderate to nearly quantitative isolated yields (Scheme 1).

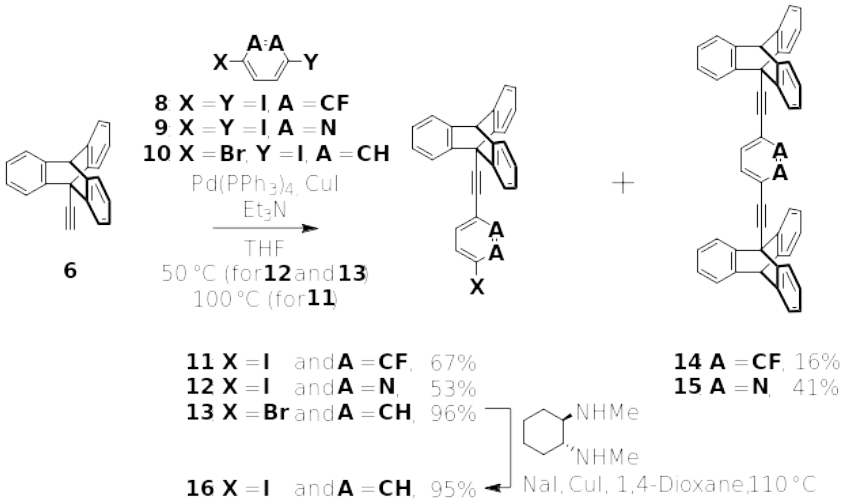

Scheme 1. Synthesis of upper molecular fragments **11**-**13** and **16**.

It was found that the combination of a triple bond substituted by a sterically demanding triptycenyl unit in **6** with the presence of substituents bulkier than a hydrogen atom in the *ortho*- position of (hetero)aryl iodides dramatically slowed down the palladium-catalyzed cross-coupling reaction. All three iodides that are known to react readily with sterically less demanding alkynes, even at room temperatureError: Reference source not found, did not show any reaction at 25 °C in this particular case. Both **9** and **10**, which have either a lone pair or hydrogen atom in the *ortho*- position, started to couple with **6** at 50 °C, but the final completion required ca. 10-40 hours. The presence of fluorine atoms in **8** retarded the coupling reaction even more, and a temperature equal to 100 °C was needed to reach the full conversion.

All attempts to couple **6** with 2,3-dichloro-1,4-diiodobenzene failed, and not even traces of product were detected by ^{1}H NMR in the crude reaction mixtures. In contrast, triptycene carrying a butadiyne unit (instead of simple acetylene as in **6**) reacted with this substrate smoothlyError: Reference source not found, clearly showing that moving the reaction center further from the triptycene unit can rule out its steric effects on the palladium-catalyzed cross-coupling reactions.

We found out that commercially available but relatively expensive **8** can be easily prepared in multigram quantities (up to 20 g), and nearly 90% isolated yield from cheap 1,2-difluorobenzene (Scheme 2). This reaction involved double *ortho*-lithiation mediated via LDA at -78 °C, followed by reaction with molecular iodine. Desired product was purified using simple vacuum distillation.

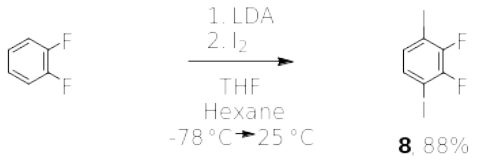

Scheme 2. Preparation of **8**.

Final assembly of **1**-**3** was achieved in four synthetic steps (Scheme 3). The first step involved Sonogashira coupling between iodides **11**, **12**, and **16**, with alkyne **7** affording double-decker structures **17**-**19** in 80-85% isolated yields. All these substrates showed nearly identical reactivity as those leading to previously discussed **11**, **12**, and **16**. The second step consisted of the TMS group removal, which was performed by TBAF in THF. All three terminal alkynes **20**-**22** were isolated in excellent yields (91-99%). It is worth mentioning that they showed notably lower solubility compared to the starting silyl derivatives. The third step introduced the carboxylic function into the molecule. This transformation consisted of the quantitative lithiation of **20**-**22** using LiHMDS at -78 °C followed by the nucleophilic addition to $ClCOOCH_3$. The esters **23** and **25** were isolated in excellent yields (97% and 88%), while the yield of **24** was somewhat lower (61%), most likely due to lower stability of the pyridazine core in the presence of lithiated alkynes.[23] The fourth step represented simple basic hydrolysis of the ester functions in **23**-**25** which afforded corresponding carboxylic acids **1**-**3** in 87-97% yields after acidic workup (Scheme 3).

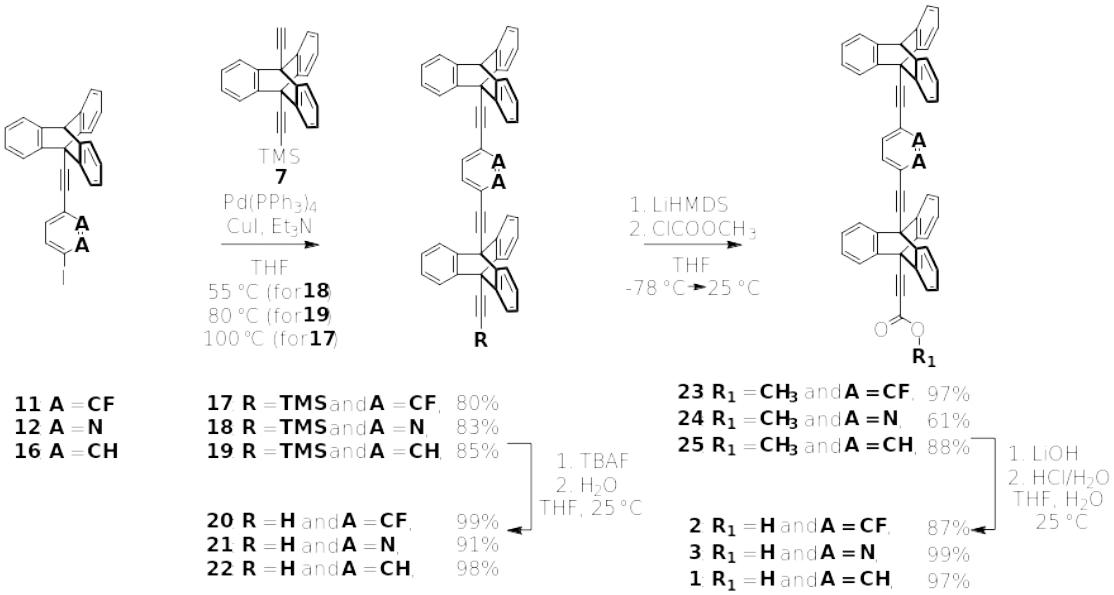

Scheme 3. Final assembly of molecular rods **1**-**3**.

Crystallography. Both molecular rods **1** and **2** afforded suitable monocrystals for X-ray diffraction in the form of colorless plates by slow diffusion of pentane into the corresponding THF solutions (Figure 1). Both compounds crystallized like solvates, and only the THF molecules were built into the crystal lattice (Figures S9 and S11 in the Supporting Information). Compound **1** crystallized in a triclinic crystal system and P-1 space group, while **2** formed monoclinic crystals with a C 2/c space group. Unfortunately, all attempts to obtain monocrystals of **3** failed.

Thorough inspection of crystal structures with a special focus on the packing properties might shed light on stacking within intended 2-D arrays. Distinct differences were found in packing between **1** and **2** that are worth mentioning. For compound **1**, both

triptycene units are nearly perfectly overlapped (they are rotated only by ~4°). The central phenyl ring leans out slightly (~12°) from the plane defined by both under- and overlaying paddles of the triptycene units (Figure 1, panel 1A). The molecule itself is nearly perfectly straight, with all triptycene bridgehead carbons, both carbon atoms of the *para*-substituted central phenyl ring, as well as almost all triple bond carbon atoms lying in one line. The only exception is the carbon atom from the carboxylic group that is tilted from this vertical axis by ~5°, mostly due to disorder (Figure 1, panel 1B).

Individual molecules whose vertical axes are oriented parallel to each other and also perpendicular to the virtual planes defined by the carboxylic acid carbon atoms are aligned in alternating rows within the crystal (Figure 2, panel 1B). Each row consists of molecules with the same orientation (either head-to-head or tail-to-tail). The intermolecular spacing (axis-to-axis) between the molecules within the same row is ~820 pm and ~740 pm between the two closest molecules from neighboring rows. The molecules within the same row are packed in such a way that two paddles of one triptycene core embrace one paddle of the neighboring triptycene unit. Such assembly resulted in the structure containing channels with rhomboidal cross-sections that are filled with five molecules of THF (Figure 2, panel 1A).

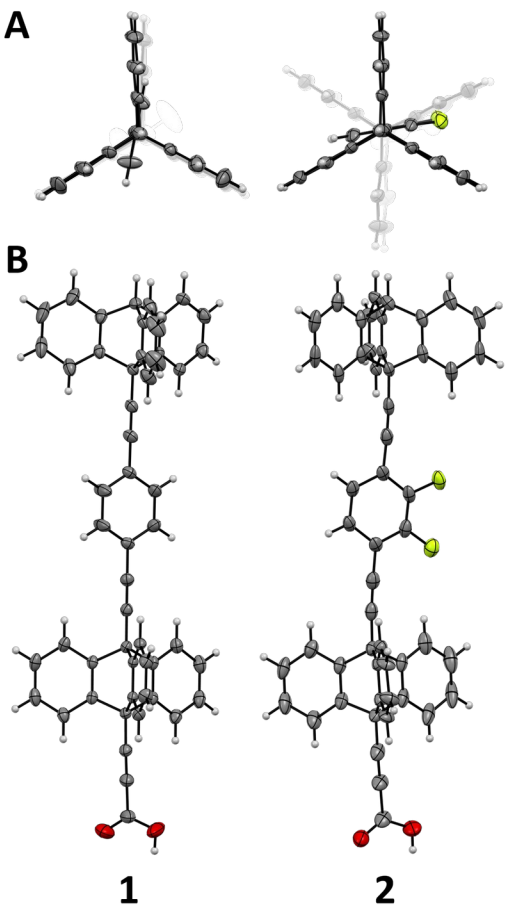

Figure 1. ORTEP visualizations of molecular rods **1** and **2**: top (A) and side (B) view. Atom labeling: hydrogen = white, carbon = gray, oxygen = red, and fluorine = yellow. Solvent molecules are omitted for clarity.

In contrast, both triptycene units that were overlapped in **1** are rotated by ~60° in compound **2** (Figure 1, panel 2A). The central difluorophenyl ring leans out by ~20° from the plane defined by one paddle of the upper triptycene unit and ~15° from the plane defined by the paddle of the lower triptycene. The whole molecule also accommodates a characteristic S-shape (Figure 1, panel 2B).

The crystal packing of **2** does not share many structural features with **1** (Figure 2). Probably the most prominent one is that the individual molecules are arranged into rows and they have the same orientation within these rows. The short list of similarities ends here. These rows are vertically shifted by ~1.1 nm towards each other (Figure 2, panel 2B). The intermolecular spacing (axis-to-axis distance) between individual molecules within one row is ~810 pm (and thus comparable to ~820 pm observed in **1**), but the inter-row separation is much smaller (~370 pm). This inter-row interaction and shifting of individual rows are clearly governed by textbook π-π interactions.[24] It was clearly identified between electronically poor difluorophenyl rings located roughly in the middle of both molecules, forming this head-to-tail oriented pair with the phenyl rings coming from the upper triptycene units. Furthermore, these rows are grouped into alternating pairs that are separated from the next pair of rows by an "interlayer" of THF molecules (Figure 2). The characteristic channels that were observed in **1** are thus absent in **2**.

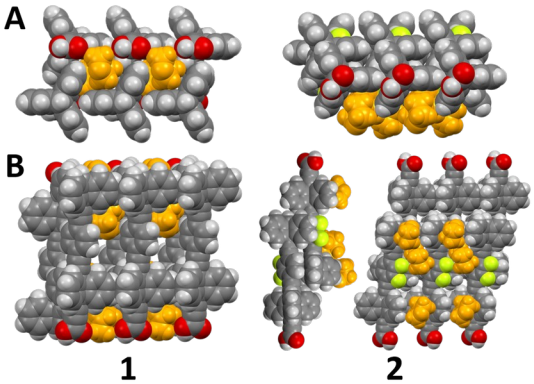

Figure 2. "Space-filling" models showing crystal packing in **1** and **2**: top (A) and side (B) views. There are two side-projections rotated by 90° along the vertical axis in the case of **2**B. Atom labelling: hydrogen = white, carbon = gray, oxygen = red, and fluorine = yellow. The THF molecules were colored in orange.

The so called "upper decks" represent another group of structurally related compounds that crystallized relatively smoothly. We were able to get suitable monocrystals of **11**, **13**, and **16** (Figure 3). Surprisingly, all attempts to get the crystal structure of **12** failed, thus revealing the relatively low tendency of the pyridazine-based rods to crystallize. The crystallographic data showed that **11** remains relatively straight with both triptycene bridgehead carbon atoms, triple bond carbon atoms and both carbon atoms of *para*-substituted phenyl ring being in one line. In contrast, both **13** and **16** were more bent (Figure 3). The centers of the phenyl rings carrying halogens are tilted by ~10° from the axis, defined by both triptycene bridgehead carbon atoms.

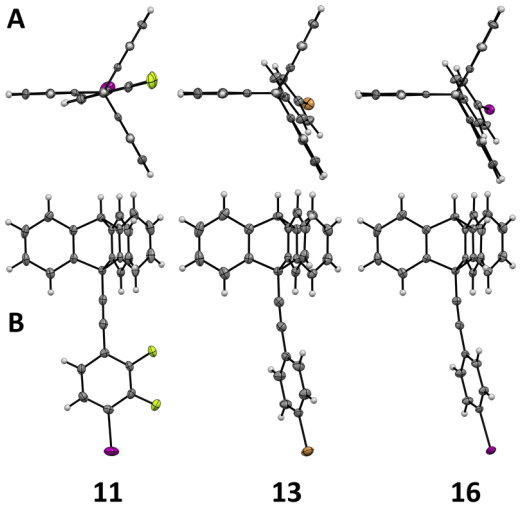

Figure 3. ORTEP visualizations of "upper decks" **11**, **13**, and **16**: top (A) and side (B) view. Atom labeling: hydrogen = white, carbon = gray, oxygen = red, fluorine = yellow, bromine = orange, and iodine = purple.

Basic crystallographic parameters of **1**, **2**, **11**, **13**, and **16** as well as packing in the crystals are listed in the Supporting Information (Table S1 and Figures S9-S18).

Acidity Constants. The prominent effect of pH on the stability of the Langmuir-Blodgett films is very well know.[25,26] The pK_a values of the newly synthesized rods **1**-**3** as well as previously known **4** and **5** were thus determined by capillary electrophoresis (Table 1). The dependences of the effective mobility of analyzed compounds on pH were measured in a series of background electrolytes within a broad pH range (0.90–5.50) at a constant temperature of 25 °C and an ionic strength equal to 25 mM. The mixed acidity constants p$K_{a,mix}$, (related to the activity of hydroxonium cations (pH)) and the actual ionic mobilities of the univalent anions of the analyzed acids, μ_{1-}, were determined from these dependences using the nonlinear regression analysis of the experimental data. Then, the mixed acidity constants, p$K_{a,mix}$, were recalculated to the thermodynamic acidity constants, p$K_{a,th}$, using the Debye-Hückel theory.[27] The mixed and thermodynamic pK_a values and the actual ionic mobilities of the analyzed compounds are presented in Table 1. The plots of dependences of the effective electrophoretic mobility of **1**-**5** on pH are shown in Figure S1.

Table 1: Acidity Constants of 1-5 Determined by Capillary Electrophoresis at 25 °C.

Cmpd.	p$K_{a,th}$ [a]	p$K_{a,mix}$ [b]	μ_{1-} [c] (10^{-9} m^2 V^{-1} s^{-1})
1	**2.53 ± 0.03**	2.46 ± 0.03	-31.04 ± 0.32
2	**2.06 ± 0.02**	1.99 ± 0.02	-30.79 ± 0.26
3	**2.36 ± 0.06**	2.29 ± 0.06	-29.26 ± 0.59
4	**2.49 ± 0.05**	2.42 ± 0.05	-29.94 ± 0.49
5	**2.85 ± 0.03**	2.78 ± 0.03	-30.64 ± 0.34

[a] The thermodynamic acidity constant related to zero ionic strength. [b] The mixed acidity constant at ionic strength at 25 mM. [c] The actual ionic mobility of the univalent anionic forms of **1**-**5**.

It was found that both molecular rods carrying a phenyl ring in the central part (structures **1** and **4**) showed nearly the same acidity (~2.50). The substitution of phenyl in **1** with pyridazine (derivative **3**) resulted in the lowering of the pK_a value to ~2.40 and formal substitution with difluorophenyl ring crowned rod **2** with the pK_a of ~2.10 as the most acidic structure from this series (Table 1). Counterintuitively, derivative **5** with a dichlorophenyl ring, which was expected to be a similarly acidic as **2**, showed in fact the lowest acidity (pK_a of ~2.90) of these five compounds. The geometrical position of the fluorine, chlorine or nitrogen atoms that are undoubtedly responsible for the changes in pK_a clearly ruled out "through-bond" interactions. The "through-space" coupling remains the only option, but the exact mechanism of action still remains unclear.

SAMs: Formation and Characterization. With all three molecular rods **1**-**3** in hand, we proceeded to the formation of the corresponding SAMs using the Langmuir-Blodgett technique. The 0.55 mM $CHCl_3$ solutions of **1**-**3** were deposited not only on pure water, but also on 10 mM aqueous solutions of LiBr, CsBr, and $Zn(NO_3)_2$ to examine the effect of cations (van der Walls radius, charge) on SAMs stability. It was found that only **1** showed noticeable sensitivity towards used cations, and the mean area per molecule (APM) that was extracted from the Langmuir-Blodgett isotherms ranged from 56 to 66 Å^2/molecule (Figure S2). Since the APMs for the remaining two rods (**2** and **3**) were not dependent on the nature of used ions but rather on their presence or absence (Figure S3-S4), $Zn(NO_3)_2$ was arbitrary chosen. The role of zinc cations was more prominent in the next step: as we reportedError: Reference source not found earlier for structurally related triptycene-based stands, the presence of Zn^{2+} ions helped to stabilize these SAMs during transfer from water surface to various solid substrates. Identical behavior was also observed for **1**-**3**. A comparison of the Langmuir-Blodgett isotherms of SAMs made of **1**-**3** is depicted in Figure 4A, with the APM ranging from 55 to 59Å^2/molecule.

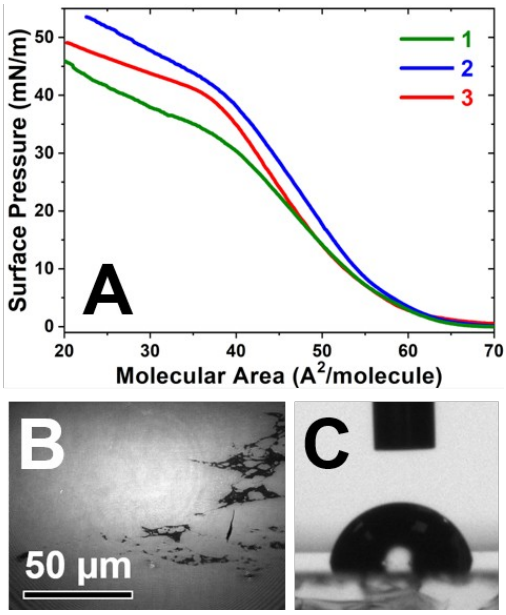

Figure 4. The Langmuir-Blodgett isotherms of **1-3** on 10 mM aqueous $Zn(NO_3)_2$ (A), structure of SAM made of **1** on aqueous $Zn(NO_3)_2$ recorded by BAM (B), and the contact angle goniometry of **1** on gold (111) (C).

All three compounds formed smoothly homogenous SAMs, as documented by images from a Brewster-angle microscope (Figure 4B – compound **1** was chosen as a representative example). These films were subsequently transferred to gold (111) surfaces using vertical dipping and characterized using standard techniques. The basic properties of individual SAMs, both on aqueous phase (APM values) and after transfer to gold (111) surfaces (ellipsometric thickness, contact angle), are summarized in Table 2.

Table 2: Area Per Molecule (Å/molecule), Contact Angle (°) and Experimental and Theoretical Monolayer Thicknesses (Å) for SAMs Made from 1-3.

Cmpd.	SAMs on 1 mM Aqueous $Zn(NO_3)_2$	SAMs on Gold (111)		
	APM ($Å^2$/molecule)	Contact Angle (°)	Experimental Monolayer Thickness (Å)	Theoretical Monolayer Thickness (Å)
1	59 ± 4	74 ± 1	18.8 ± 1.6	24.0
2	59 ± 2	75 ± 2	19.5 ± 1.9	24.0
3	55 ± 3	77 ± 4	18.9 ± 0.5	24.0

The presence of characteristic infrared vibrations of **1**, **2** or **3** within corresponding SAMs on the gold (111) surface was unequivocally confirmed using polarization modulation-infrared reflection absorption spectroscopy (PM-IRRAS). Comparison of the isotropic IR spectrum of **1** (acquired in KBr) with the anisotropic spectrum of corresponding SAM transferred to gold (111) substrate is depicted in Figure 5 (spectra of **2** and **3** are shown in Figures S7 and S8). Both the isotropic and anisotropic spectra are sharing several features. Starting from higher frequencies, the C-H stretches of phenyl rings are clearly visible at ~3070 and ~3020 cm^{-1}. The sharp vibration at ~2957 cm^{-1} was assigned to C-H stretching of the bridgehead hydrogen atom. The anisotropic spectrum of **1** (Figure 5) also contains some aliphatic symmetric and asymmetric vibrations (marked with blue asterisks) that are due to common atmospheric contaminants, which has been reported earlier.[28] The weakly polarized carbon-substituted triple bonds $\nu(C \equiv C)$ are easily identifiable at ~2240 cm^{-1}. The C=O stretches of the free (~1730 cm^{-1}) and dimeric form (~1700 cm^{-1}) of carboxylic function as well as the C=C stretches of phenyl rings (~1607 cm^{-1}) are well separated in the isotropic spectrum, but collapse into one rather broad peak centered at ~1660 cm^{-1} in the anisotropic spectrum. Due to optical properties of the gold (111) substrate the identification of peaks below ~1400 cm^{-1} in PM-IRRAS spectra becomes increasingly difficult and was not attempted. The absence of sufficient amount of well-resolved and properly polarized vibrations (parallel vs perpendicular to the surface) unfortunately did not allow us for determination of molecular tilting.Error: Reference source not found

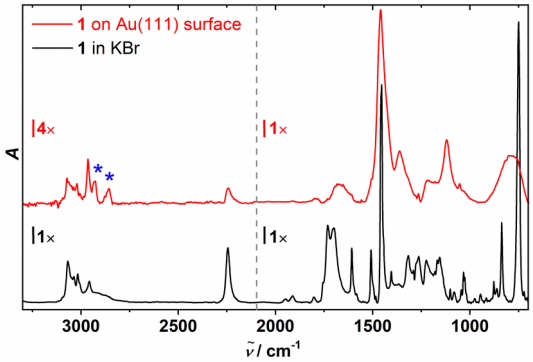

Figure 5. Infrared spectra of **1**: isotropic in the KBr (black solid line) and anisotropic PM-IRRAS spectrum of corresponding SAMs (red solid line) on gold surface. Blue asterisks indicate common atmospheric contaminants.

The experimentally obtained monolayer thickness reached ∼19 Å in all three cases, while the theoretical models considering perpendicular orientation of individual molecules (including zinc cations) towards surface predicted ∼24 Å. This obvious discrepancy can be explained by tilting and possibly also by bending. The application of a simple trigonometric function suggests tilting of ∼38°, which agrees with previous observations.Error: Reference source not found Molecules were considered as solid rods, and bending was thus omitted in this simple approximation. It is worth mentioning that not only tilting and/or bending can affect the experimentally obtained monolayer thickness, but surface roughness and the index of refraction that was arbitrarily set as 1.47 (based on our previous experiences)Error: Reference source not found should also be considered. However, their impact on averaged monolayer thickness is usually less prominent.

Another piece of information regarding the texture of these films can provide APM. This value ranges from 55 to 59 Å/molecule for **1**-**3** (Table 2), and Figure 6 shows two possible polymorphs whose APMs nicely overlap with these experimental data. In particular, polymorph A (Figure 5) was observed earlier in the triptycene-based "monodecker"Error: Reference source not found as well as "double-decker"Error: Reference source not found structures. It is thus believed that this packing motive is more general within triptycene-based SAMs. However, the absence of crystallographic data cannot exclude polymorph B from consideration.

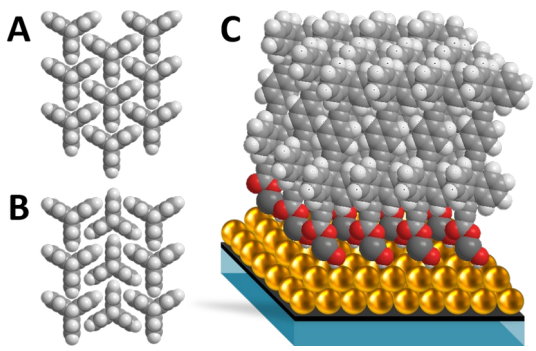

Figure 6. SAMs: top views on structures of two possible polymorphs (A) and (B), and proposed structure of SAM made of **1** on gold (111) surface (C).

Detailed structural analysis of these SAMs on various surfaces including advanced molecular dynamic simulations as well as static DFT optimizations will be reported in the more field-specific journal soon.

SUMMARY

Three molecular rods **1**-**3** that represent shorter and stiffer analogs to two already known structures **4** and **5** were designed and synthesized. The whole synthetic scheme is modular and allows for the introduction of different linkers into the rigid molecular backbone. However, the bulkiness of the triptycene unit in combination with the ethynyl group(s) present on its bridgehead atom(s) also sets limits on reactivity, and thus slightly reduces the pool of available substrates that are tolerated. All three rods **1**-**3** formed sturdy SAMs on the water-air interface using Langmuir-Blodgett technique with the mean area per molecule 55-59 $Å^2$/molecule. These values correspond with expected tight triptycene packing. The thickness of all three SAMs reaches ~19 Å after transfer to a gold (111) surface, meaning that individual molecules are tilted maximally 38° from the axis perpendicular to the surface. Such "double-decker" systems are thus promising platforms for carrying various molecular machines which can be installed on the top of the upper triptycene unit.

EXPERIMENTAL SECTION

Materials. All reactions were carried out under argon atmosphere with dry solvents freshly distilled under anhydrous conditions, unless otherwise noted. Standard Schlenk and vacuum line techniques were employed for all manipulations of air- or moisture-sensitive compounds. Yields refer to isolated, chromatographically and spectroscopically homogenous materials, unless otherwise stated.

9-Ethynyltriptycene (**6**),Error: Reference source not found and 9-trimethylsilylethynyl-10-ethynyltriptycene (**7**)Error: Reference source not found were synthesized according to the previously published procedures. THF and ether were dried over sodium with benzophenone and distilled under argon prior to use. 1,4-Dioxane was dried over sodium and distilled under argon prior to use. Triethylamine and diisopropylamine were dried over CaH_2 and distilled under argon prior to use. All other reagents were used as supplied unless otherwise stated.

Procedures. Analytical thin-layer chromatography (TLC) was performed using precoated TLC aluminum sheets (Silica gel 60 F_{254}). TLC spots were visualized using either UV light (254 nm) or a 5% solution of phosphomolybdic acid in ethanol, and heat (200 °C) as a developing agent. Flash chromatography was performed using silica gel (high purity grade, pore size 60 Å, 70 - 230 mesh). Melting points are reported uncorrected. Infrared spectra (IR) were recorded in KBr pellets. Chemical shifts in ^{1}H, ^{13}C, and ^{19}F NMR spectra are reported in ppm on the δ scale relative to $CHCl_3$ (δ = 7.26 ppm for ^{1}H NMR), $CHCl_3$ (δ = 77.0 ppm for ^{13}C NMR), THF-d_8 (δ = 1.72 and 3.58 ppm for ^{1}H NMR), and THF-d_8 (δ = 25.40 and 67.50 ppm for ^{13}C NMR), as internal references. Splitting patterns are assigned s = singlet, d = doublet, t = triplet, m = multiplet, br = broad signal. The volume/volume (v/v) ratios of solvents were used to prepare mobile phases for column chromatographies.

High-resolution mass spectra (HRMS) using atmospheric-pressure chemical ionization (APCI) and electrospray ionization (ESI) were obtained on a mass analyzer combining linear ion trap and the Orbitrap, and those using chemical ionization (CI) mode were taken on a time-of-flight mass spectrometer.

X-ray Diffraction. Crystallographic data for **11**, **13**, and **16** were collected on Nonius Kappa CCD diffractometer equipped with Bruker APEX-II CCD detector by monochromatized MoK_{α} radiation (λ = 0.71073 Å) at a temperature of 150(2) K. The structures were solved by direct methods (SHELXS)[29] and refined by full matrix least squares based on F^2 (SHELXL97).Error: Reference source not found

Measurements of pK_a. Capillary electrophoresis (CE) measurements were conducted on CE 7100 analyzer (Agilent, Waldbronn, Germany) in internally untreated fused silica capillary with outer polyimide coating (id/od 50/375 µm, total/effective (to the detector) length 480/395 mm, Polymicro Technologies, Phoenix, AZ, USA). The analyzed compounds were detected by on-column UV-vis spectrophotometric diode array detector set at 200 nm.

Ellipsometry. For all compounds, the ellipsometric thickness was determined by analyzing three samples and doing five measurements per sample, using the Variable Angle Stokes Ellipsometer (Geartner Scientific, USA). A value of 1.47 was used as the index of refraction, based on previous work.Error: Reference source not found

Contact Angle Goniometry. For each tested compound, at least four contact angle measurements across two samples were carried out. The CAM 101 Contact Angle Goniometer (KSV Instruments Ltd., Finland) was used for these measurements.

Polarization Modulation-Infrared Reflection Absorption Spectroscopy (PM-IRRAS). Infrared spectra were recorded on freshly produced SAMs immediately after transfer from water surface to gold (111) substrates. The acquisition time was 4.5 hours (6000 scans), during which the detector was cooled with liquid nitrogen. At least five spectra per compound were recorded. The raw data was background subtracted and baseline corrected. The Polarization-Modulation Infrared Reflection Absorption Spectrometer (Thermo Fisher Scientific, USA) was used for these experiments.

General procedure for basic ester hydrolysis (GP 1). To a solution of esters **28**, **29**, and **30** (1.0 equiv.) in THF (15 mL) was added a solution of $LiOH.H_2O$ (5.0 equiv.) in water (5 mL) at room temperature. The clear yellowish mixture was stirred for 3 h at room temperature. THF was removed under reduced pressure and the white suspension was diluted with water (5 mL). The aqueous phase was acidified with concentrated HCl (pH ≈ 1), a dense white precipitate was filtered on a frit, subsequently washed with deionized water (3 × 10 mL), hexane (3 × 20 mL), ether (1 × 5 mL), and finally thoroughly dried using Kugelrohr distillation apparatus (60 min, 80 °C, 500 mTorr). Molecular rods **1**, **2**, and **3** were obtained as white crystalline solids.

Rod 1 was prepared from ester **25** (250 mg, 0.351 mmol, 1.0 equiv.) in THF (20 mL), and $LiOH.H_2O$ (74 mg, 1.754 mmol, 5.0 equiv.) in water (5 mL) according to **GP1**. Rod **1** was obtained as a white crystalline solid (237 mg, 0.339 mmol, 97%).

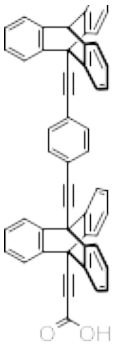

Mp > 300 °C (dec.). ^{1}H NMR (500 MHz, THF-d_8): δ 5.57 (s, 1H), 7.02 – 7.08 (m, 6H), 7.15 – 7.17 (m, 6H), 7.42 – 7.44 (m, 3H), 7.74 – 7.75 (m, 3H), 7.81 – 7.82 (m, 3H), 7.87 – 7.89 (m, 3H), 8.03 (s, 4H). ^{13}C {^{1}H} NMR (125 MHz, THF-d_8): δ 53.2, 54.05, 54.14, 54.7, 80.6, 86.0, 86.6, 87.2, 93.3, 94.0, 122.9, 123.1, 123.4, 124.0, 124.4, 124.6, 125.9, 126.6, 126.9, 127.0, 133.3, 143.6, 144.4, 145.5, 145.9, 154.4. IR (KBr): 3426, 3068, 3037, 3017, 2957, 2245, 1731, 1700, 1607, 1509, 1454, 1404, 1316, 1263, 1224, 1179, 1168, 1155, 1101, 1081, 1044, 1032, 1027, 975, 945, 877, 861, 836, 749, 672, 655, 640, 607, 553, 546, 522, 481 cm^{-1}. MS, *m/z* (%): 699.2 (10, M + H), 655.2 (100, M – COOH). HRMS, (APCI) for ($C_{53}H_{30}O_2$ + H^+): calcd

699.2319, found 699.2319. Anal. Calcd. for $C_{53}H_{30}O_2$: C, 91.09; H, 4.33. Found: C, 91.17; H, 4.30.

Rod 2 was prepared from ester **23** (130 mg, 0.174 mmol, 1.0 equiv.) in THF (15 mL), and LiOH.H_2O (37 mg, 0.870 mmol, 5.0 equiv.) in water (5 mL) according to **GP1**. Rod **2** was obtained as a white crystalline solid (113 mg, 0.152 mmol, 87%).

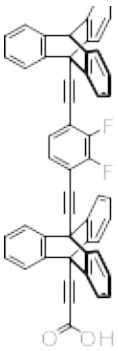

Mp > 260 °C (dec.). ^{1}H NMR (500 MHz, THF-d_8): δ 5.59 (s, 1H), 7.03 – 7.09 (m, 6H), 7.17 – 7.19 (m, 6H), 7.44 – 7.45 (m, 3H), 7.76 – 7.77 (m, 3H), 7.80 – 7.82 (m, 3H), 7.87 – 7.88 (m, 5H). ^{13}C {^{1}H} NMR (125 MHz, THF-d_8): δ 53.2, 54.1, 54.2, 54.9, 80.4, 85.4 (m), 86.1 (m), 86.8, 92.7 (m), 94.0 (m), 114.8 (dd, $J_{C,F}$ = 4 Hz, $J_{C,F}$ = 10 Hz), 115.4 (dd, $J_{C,F}$ = 7 Hz, $J_{C,F}$ = 8 Hz), 122.99, 123.02, 123.2, 124.5, 126.0, 126.7, 127.08, 127.13, 129.6 (m), 143.5, 144.0, 145.1, 145.8, 152.66 (dd, $^2J_{C,F}$ = 15 Hz, $^1J_{C,F}$ = 255 Hz), 152.72 (dd, $^2J_{C,F}$ = 15 Hz, $^1J_{C,F}$ = 255 Hz), 154.3. ^{19}F NMR (470 MHz, THF-d_8): δ -260.98 - -260.97 (m, 2F). IR (KBr): 3429, 3068, 3018, 2959, 2245, 1729, 1696, 1623, 1607, 1555, 1500, 1473, 1457, 1402, 1363, 1323, 1302, 1290, 1266, 1235, 1191, 1166, 1096, 1071, 1057, 1033, 1027, 986, 943, 868, 822, 749, 717, 695, 681, 669, 658, 640, 629, 619, 607, 526, 512, 486 cm^{-1}. MS, *m/z* (%): 691.2 (100, M + H). HRMS, (APCI) for ($C_{53}H_{28}F_2O_2$ + H^+): calcd 735.2130, found 735.2134. Anal. Calcd. for $C_{53}H_{28}F_2O_2$ + THF in 1:1 ratio: C, 84.85; H, 4.50. Found: C, 84.60; H, 4.25.

Rod 3 was prepared from ester **24** (100 mg, 0.140 mmol, 1.0 equiv.) in THF (15 mL), and LiOH.H_2O (29 mg, 0.700 mmol, 5.0 equiv.) in water (5 mL) according to **GP1**. Rod **3** was obtained as a white crystalline solid (97 mg, 0.138 mmol, 99%).

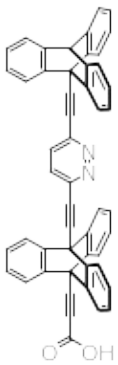

Mp > 240 °C (dec.). ^{1}H NMR (500 MHz, THF-d_8): δ 5.59 (s, 1H), 7.04 – 7.10 (m, 6H), 7.16 – 7.20 (m, 6H), 7.44 – 7.46 (m, 3H), 7.76 – 7.77 (m, 3H), 7.86 – 7.88 (m, 3H), 7.93 – 7.94 (m, 3H), 8.27 (s, 1H), 8.28 (s, 1H). ^{13}C {^{1}H} NMR (125 MHz, THF-d_8): δ 53.2, 54.0, 54.2, 54.7, 80.5, 86.7, 89.5, 90.8, 91.0, 91.6, 123.0, 123.1, 123.4, 124.5, 126.1, 126.8, 127.1, 127.2, 130.37, 130.38, 143.5, 143.9, 145.0, 145.8, 146.8, 147.2, 154.3. IR (KBr): 3068, 3017, 2959, 2243, 1710, 1607, 1531, 1457, 1405, 1314, 1261, 1226, 1213, 1194, 1170, 1156, 1033, 945, 877, 848, 829, 750, 691, 674, 640, 616, 608, 587, 573, 552, 480 cm^{-1}. MS, *m/z* (%): 723.5 (20, M + Na), 701.5 (100, M + H). HRMS, (ESI+) for ($C_{51}H_{28}N_2O_2$ + H^+): calcd 701.2224, found 701.2221. Anal. Calcd. for $C_{51}H_{28}N_2O_2$: C, 87.41; H, 4.03; N, 4.00. Found: C, 87.25; H, 4.10; N, 3.75.

2,3-Difluoro-1,4-diiodobenzene (**8**). To the well-stirred solution of *i*-Pr_2NH (16.4 mL, 116.7 mmol, 2.3 equiv.) in THF (100 mL) was slowly added the solution of *n*-BuLi in hexane (1.6 M, 66.6 mL, 106.6 mmol, 2.1 equiv.) during 15 min at -78 °C. Subsequently, 1,2-difluorobenzene (5.00 mL, 50.7 mmol, 1.0 equiv.) was added to the colorless solution from a syringe and the reaction mixture was stirred at that temperature for next 5 h. White solid precipitated during that time. The mixture was treated with a precooled solution (-78 °C) of iodine (28.3 g, 111.6 mmol, 2.2 equiv.) in THF (100 mL) and the deeply red solution was stirred at that temperature for an additional 20 min. Cooling was discontinued, the dark solution was slowly warmed to room temperature, diluted with ether (400 mL) and subsequently washed with concentrated aqueous $Na_2S_2O_3$ (2 × 80 mL), 15% aqueous HCl (2 × 100 mL), and 15% aqueous $NaHCO_3$ (1 × 50 mL). The clear colorless organic phase was dried over $MgSO_4$. Solvents were removed under reduced pressure and distillation of the yellow oily residue on Kugelrohr distillation apparatus

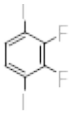

(150 °C, 600 mTorr) gave **8** as a slightly yellowish oil which immediately crystallized (16.3 g, 44.6 mmol, 88%).

Mp 56.4 – 57.5 °C. ^{1}H NMR (400 MHz, $CDCl_3$): δ 7.25 – 7.26 (m, 2H). ^{13}C {^{1}H} NMR (100 MHz, $CDCl_3$): δ 82.3 (m), 134.9 (m), 150.0 (dd, $^{2}J_{C,F}$ = 18 Hz, $^{1}J_{C,F}$ = 253 Hz). ^{19}F NMR (376 MHz, $CDCl_3$):δ -236.64 (dd, J_1 = 1 Hz, J_2 = 2 Hz, 2F). IR (KBr): 1448, 1281, 1253, 1229, 1146, 1116, 870, 865, 796, 792, 612, 597, 542 cm^{-1}. MS, *m/z* (%): 366.8 (95, M + H), 239.9 (100, M – I + H). HRMS, (CI) for ($C_6H_2F_2I_2$ + H^+): calcd 366.8292, found 366.8289. Anal. Calcd. for $C_6H_2F_2I_2$: C, 19.70; H, 0.55. Found: C, 19.91; H, 0.68, which agrees with the literature.[30]

9-((2,3-Difluoro-4-iodophenyl)ethynyl)triptycene (**11**). A flame-dried 50 mL two necked flask equipped with a stir bar and gas condenser was charged with alkyne **6** (600 mg, 2.156 mmol, 1.0 equiv.), 2,3-difluoro-1,4-diiodobenzene (**8**) (3.155 g, 8.624 mmol, 4.0 equiv.), $Pd(PPh_3)_4$ (100 mg, 0.086 mmol, 4 mol %), and CuI (12 mg, 0.065 mmol, 3 mol %). After five successive vacuum/argon cycles, degassed dry THF (10 mL) and triethylamine (10 mL) were added from a syringe. The slightly yellowish solution was refluxed for 10 h at the temperature of the oil bath 100 °C and 16 h at 80 °C. A dense white solid precipitated. Progress of the reaction was monitored by the ^{1}H and ^{19}F NMR. The crude reaction mixture was cooled to room temperature, diluted with CH_2Cl_2 (100 mL) and washed with saturated aqueous NH_4Cl (2 × 30 mL). The clear yellowish organic phase was dried over $MgSO_4$ and volatiles were removed under reduced pressure. Column chromatography on silica gel (hexane/CH_2Cl_2 - 5:1) gave **11** as a white crystalline solid (742 mg, 1.437 mmol, 67%).

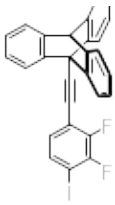

Mp 284.0 – 285.4 °C. ^{1}H NMR (400 MHz, $CDCl_3$): δ 5.48 (s, 1H), 7.06 – 7.12 (m, 6H), 7.34 (ddd, J_1 = 1.79 Hz, J_2 = 6.20 Hz, J_3 = 8.19 Hz, 1H), 7.43 – 7.45 (m, 3H), 7.60 (ddd, J_1 = 1.88 Hz, J_2 = 5.51 Hz, J_3 = 8.27 Hz, 1H), 7.78 – 7.80 (m, 3H). ^{13}C {^{1}H} NMR (100 MHz, $CDCl_3$): δ 53.3, 53.7, 83.1 (d, $J_{C,F}$ = 22 Hz), 84.1 (d, $J_{C,F}$ = 4 Hz), 92.0 (d, $J_{C,F}$ = 4 Hz), 114.0 (dd, $J_{C,F}$ = 1 Hz, $J_{C,F}$ = 13 Hz), 122.3, 123.5, 125.3, 125.9, 129.3 (d, $J_{C,F}$ = 4 Hz), 133.5 (dd, $J_{C,F}$ = 1 Hz, $J_{C,F}$ = 5 Hz), 143.8, 144.3, 150.8 (dd, $^{2}J_{C,F}$ = 15 Hz, $^{1}J_{C,F}$ = 255 Hz), 150.9 (dd, $^{2}J_{C,F}$ = 15 Hz, $^{1}J_{C,F}$ = 251 Hz). ^{19}F NMR (376 MHz, $CDCl_3$):δ -253.95 (ddd, J_1 = 2 Hz, J_2 = 6 Hz, J_3 = 22 Hz, 1F), -239.56 (ddd, J_1 = 2 Hz, J_2 = 5 Hz, J_3 = 22 Hz, 1F). IR (KBr): 3059, 3035, 3019, 2961, 2917, 2849, 2241, 1606, 1558, 1485, 1475, 1453, 1325, 1291, 1230, 1183, 1120, 1067, 1025, 962, 914, 871, 812, 758, 718, 694, 682, 641, 629, 607, 590, 540, 525, 481 cm^{-1}. MS, *m/z* (%): 517.0 (100, M + H). HRMS, (APCI) for ($C_{28}H_{15}F_2I$ + H^+): calcd 517.0259, found 517.0260. Anal. Calcd. for $C_{28}H_{15}F_2I$: C, 65.13; H, 2.93. Found: C, 64.86; H, 2.99.

9-((6-Iodopyridazinyl)ethynyl)triptycene (**12**). A flame-dried Schlenk flask was charged with alkyne **6** (600 mg, 2.156 mmol, 1.0 equiv.), 3,6-diiodopyridazine (**9**) (2.862 g, 8.624 mmol, 4.0 equiv.), $Pd(PPh_3)_4$ (100 mg, 0.086 mmol, 4 mol %), and CuI (12 mg, 0.065 mmol, 3 mol %). After three successive vacuum/argon cycles, degassed dry THF (15 mL) and triethylamine (10 mL) were added from a syringe. The slightly yellowish solution was stirred for 36 h at the temperature of the oil bath 50 °C. A dense white solid precipitated. Progress of the reaction was checked in 8 h intervals by ^{1}H NMR. If the alkyne **6** was still present, additional portion of $Pd(PPh_3)_4$ (80 mg, 0.069 mmol) and CuI (20 mg, 0.105 mmol) were added and heating was continued. The crude reaction mixture was diluted with CH_2Cl_2 (250 mL) and washed with saturated aqueous NH_4Cl (2 × 30 mL). The clear yellowish organic phase was dried over $MgSO_4$ and volatiles were removed under reduced pressure. Five times repeated column chromatography

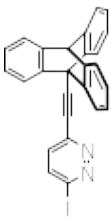

on silica gel (hexane/acetone - 4:1) gave **12** as a white crystalline solid (556 mg, 1.153 mmol, 53%).

Mp > 180 °C (dec.). ^{1}H NMR (400 MHz, $CDCl_3$): δ 5.47 (s, 1H), 7.06 – 7.09 (m, 6H), 7.42 – 7.44 (m, 3H), 7.53 (d, J = 8.67 Hz, 1H), 7.78 – 7.81 (m, 3H), 7.93 (d, J = 8.67 Hz, 1H). ^{13}C {^{1}H} NMR (100 MHz, $CDCl_3$): δ 53.2, 53.5, 88.4, 91.0, 122.3, 123.5, 123.6, 125.3, 126.0, 130.5, 136.6, 143.4, 144.2, 146.9. IR (KBr): 3065, 3050, 3036, 3017, 3001, 2960, 2924, 2246, 1609, 1552, 1511, 1457, 1438, 1403, 1388, 1323, 1290, 1267, 1211, 1172, 1154, 1130, 1100, 1068, 1022, 977, 940, 916, 876, 852, 797, 751, 701, 641, 607, 546, 536, 486 cm^{-1}. MS, *m/z* (%): 505.1 (100, M + Na), 483.1 (65, M + H). HRMS, (ESI+) for ($C_{26}H_{15}{}^{127}IN_2$ + H^+): calcd 483.0353, found 483.0344. Anal. Calcd. for $C_{26}H_{15}IN_2$ + CH_2Cl_2 in 8:1 ratio: C, 63.66; H, 3.12; N, 5.68. Found: C, 63.60; H, 3.22; N, 5.84.

9-((4-Bromophenyl)ethynyl)triptycene (**13**). A flame-dried Schlenk flask was charged with alkyne **6** (600 mg, 2.156 mmol, 1.0 equiv.), 1-bromo-4-iodobenzene (**10**) (732 mg, 2.587 mmol, 1.2 equiv.), $Pd(PPh_3)_4$ (100 mg, 0.086 mmol, 4 mol %), and CuI (12 mg, 0.065 mmol, 3 mol %). After three successive vacuum/argon cycles, degassed dry THF (10 mL) and triethylamine (10 mL) were added from a syringe. The slightly yellowish solution was stirred for 10 h at 50 °C. A dense white solid precipitated. A crude reaction mixture was diluted with CH_2Cl_2 (100 mL) and washed with saturated aqueous NH_4Cl (2 × 30 mL). A clear yellowish organic phase was dried over $MgSO_4$ and volatiles were removed under reduced pressure. Column chromatography on silica gel (hexane/CH_2Cl_2, 5:1) provided **13** as a white crystalline solid (897 mg, 2.070 mmol, 96%).

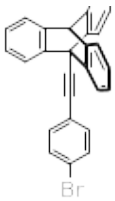

Mp 290.3 – 292.5 °C. ^{1}H NMR (400 MHz, $CDCl_3$): δ 5.45 (s, 1H), 7.04 – 7.10 (m, 6H), 7.41 – 7.43 (m, 3H), 7.61 – 7.63 (m, 2H), 7.68 – 7.71 (m, 2H), 7.77 – 7.79 (m, 3H). ^{13}C {^{1}H} NMR (100 MHz, $CDCl_3$): δ 53.3, 53.5, 85.1, 91.6, 121.9, 122.4, 123.0, 123.5, 125.2, 125.8, 131.8, 133.5, 144.2, 144.4. IR (KBr): 3063, 3039, 3018, 2962, 2241, 1610, 1587, 1487, 1458, 1392, 1316, 1291, 1277, 1173, 1146, 1128, 1108, 1093, 1072, 1024, 1011, 947, 937, 916, 875, 857, 822, 816, 783, 759, 747, 698, 641, 635, 608, 538, 515, 482 cm^{-1}. MS, *m/z* (%): 432.1 (100, M, centre of isotope cluster), 352.1 (46, M – Br), 276.1 (14), 252.1 (23), 175.1 (11). HRMS, (EI) for ($C_{28}H_{17}Br^+$): calcd 432.0514, found 432.0513. Anal. Calcd. for $C_{28}H_{17}Br$: C, 77.61; H, 3.95. Found: C, 77.39; H, 3.91.

Compound 14 was isolated as a more polar side product during the chromatography of **11** described above using more polar mobile phase (hexane/CH_2Cl_2 – 1:1) as a white crystalline solid (231 mg, 0.346 mmol, 16%).

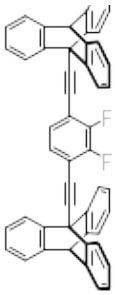

Mp > 300 °C (dec.). ^{1}H NMR (400 MHz, $CDCl_3$): δ 5.49 (s, 2H), 7.07 – 7.15 (m, 12H), 7.44 – 7.46 (m, 6H), 7.66 (dd, J_1 = 1.41 Hz, J_2 = 2.71 Hz), 7.84 – 7.86 (m, 6H). ^{13}C {^{1}H} NMR (100 MHz, $CDCl_3$): δ 53.3, 53.8, 84.5 (m), 92.6 (m), 114.2 (dd, $J_{C,F}$ = 6 H, $J_{C,F}$ = 9 Hz), 122.4, 123.6, 125.3, 125.9, 128.1 (m), 143.9, 144.3, 151.8 (dd, $^{2}J_{C,F}$ = 15 Hz, $^{1}J_{C,F}$ = 256 Hz). ^{19}F NMR (376 MHz, $CDCl_3$): δ -256.99 (dd, J_1 = 2 Hz, J_2 = 3 Hz, 2F). IR (KBr): 3066, 3016, 2952, 2241, 1608, 1551, 1499, 1473, 1457, 1321, 1289, 1263, 1227, 1183, 1155, 1076, 1065, 1027, 985, 941, 910, 869, 813, 745, 688, 677, 641, 605, 531, 525, 481 cm^{-1}. MS, *m/z* (%): 667.2 (100, M + H). HRMS, (APCI) for ($C_{50}H_{28}F_2$ + H^+): calcd 667.2232, found 667.2233. Anal. Calcd. for $C_{50}H_{28}F_2$ + CH_2Cl_2 in 3:2 ratio: C, 84.13; H, 4.09. Found: C, 84.39; H, 4.10.

Compound 15 was isolated as a more polar side product during the chromatography of **12** described above using more polar mobile phase (CH_2Cl_2) as a white crystalline solid (280 mg, 0.443 mmol, 41%).

Mp > 300 °C (dec.). ^{1}H NMR (400 MHz, $CDCl_3$): δ 5.49 (s, 2H), 7.08 – 7.14 (m, 12H), 7.44 – 7.45 (m, 6H), 7.87 – 7.89 (m, 6H), 8.04 (s, 2H). ^{13}C {^{1}H} NMR (100 MHz, $CDCl_3$): δ 53.3, 53.6, 89.0, 91.7, 122.5, 123.7, 125.4, 126.0, 129.7, 143.5, 144.3, 146.1. IR (KBr): 3069, 3017, 2960, 2248, 1608, 1523, 1458, 1406, 1310, 1290, 1279, 1173, 1156, 1143, 1026, 877, 847, 751, 685, 641, 607, 482 cm^{-1}. MS, *m/z* (%): 655.3 (100, M + Na), 633.3 (80, M + H). HRMS, (ESI+) for ($C_{48}H_{28}N_2$ + H^+): calcd 633.2325, found 633.2317. Anal. Calcd. for $C_{48}H_{28}N_2$ + CH_2Cl_2 in 6:1 ratio: C, 89.43; H, 4.41; N, 4.33. Found: C, 89.17; H, 4.27; N, 3.97.

9-((4-Iodophenyl)ethynyl)triptycene (**16**). A flame-dried Schlenk flask was charged with **13** (600 mg, 1.385 mmol, 1.0 equiv.), dry NaI (415 mg, 2.769 mmol, 2.0 equiv.), and CuI (13 mg, 0.069 mmol, 5 mol %). After three successive vacuum/argon cycles, degassed dry 1,4-dioxane (2.50 mL) and racemic *trans-N,N´*-dimethyl-1,2-cyclohexanediamine (18 µL, 0.139 mmol, 10 mol %) were added. A yellowish suspension was stirred at 110 °C for 36 h, allowed to reach room temperature, diluted with CH_2Cl_2 (100 mL), and washed with saturated aqueous NH_4Cl (2 × 30 mL). The clear yellowish organic phase was dried over $MgSO_4$ and volatiles were removed under reduced pressure. Column chromatography on silica gel (hexane/CH_2Cl_2 - 4:1) yielded **16** as a white crystalline solid (632 mg, 1.316 mmol, 95%).

Mp 291.8 – 292.9 °C. ^{1}H NMR (400 MHz, $CDCl_3$): δ 5.45 (s, 1H), 7.04 – 7.10 (m, 6H), 7.41 – 7.43 (m, 3H), 7.54 – 7.57 (m, 2H), 7.76 – 7.78 (m, 3H), 7.81 – 7.84 (m, 2H). ^{13}C {^{1}H} NMR (100 MHz, $CDCl_3$): δ 53.3, 53.5, 85.4, 91.8, 94.6, 122.39, 122.44, 123.5, 125.2, 125.7, 133.6, 137.7, 144.2, 144.4. IR (KBr): 3064, 3037, 3017, 2962, 2239, 1609, 1582, 1485, 1457, 1390, 1315, 1290, 1276, 1181, 1172, 1108, 1059, 1025, 1008, 947, 875, 816, 779, 758, 748, 697, 641, 635, 607, 534, 515, 486, 481 cm^{-1}. MS, *m/z* (%): 480.0 (100, M), 352.1 (24, M – I), 276.1 (8), 252.1 (17), 175.1 (10), 126.9 (5, I). HRMS, (EI) for ($C_{28}H_{17}I^+$): calcd 480.0375, found 480.0377. Anal. Calcd. for $C_{28}H_{17}I$: C, 70.01; H, 3.57. Found: C, 69.78; H, 3.57.

Compound 17. A flame-dried 50 mL two necked flask equipped with a stir bar and gas condenser was charged with iodide **11** (350 mg, 0.678 mmol, 1.0 equiv.), alkyne **7** (330 mg, 0.881 mmol, 1.3 equiv.), $Pd(PPh_3)_4$ (31 mg, 0.027 mmol, 4 mol %), and CuI (4 mg, 0.020 mmol, 3 mol %). After five successive vacuum/argon cycles, degassed dry THF (10 mL) and triethylamine (10 mL) were added from a syringe. The slightly yellowish solution was refluxed for 4 h at the temperature of the oil bath 100 °C. A dense white solid precipitated. Progress of the reaction was monitored by the ^{1}H and ^{19}F NMR. The crude reaction mixture was cooled to room temperature, diluted with CH_2Cl_2 (100 mL) and washed with saturated aqueous NH_4Cl (2 × 30 mL). The clear yellowish organic phase was dried over $MgSO_4$ and volatiles were removed under reduced pressure. Column chromatography on silica gel (hexane/CH_2Cl_2 - 3:1) gave **17** as a white crystalline solid (415 mg, 0.544 mmol, 80%).

Mp > 300 °C (dec.). ^{1}H NMR (400 MHz, $CDCl_3$): δ 0.51 (s, 9H), 5.50 (s, 1H), 7.08 – 7.16 (m, 6H), 7.17 – 7.19 (m, 6H), 7.45 – 7.47 (m, 3H), 7.67 (s, 1H), 7.68 (s, 1H), 7.80 – 7.82 (m, 3H), 7.86 – 7.88 (m, 6H). ^{13}C {^{1}H} NMR (100 MHz, $CDCl_3$): δ 0.3, 53.06, 53.10, 53.3, 53.81, 84.5 (m), 84.9 (m), 92.2 (d, $J_{C,F}$ = 3 Hz), 92.7 (d, $J_{C,F}$ = 3 Hz), 98.3, 99.4, 114.0 (dd, $J_{C,F}$ = 4 Hz, $J_{C,F}$ = 11 Hz), 114.3 (dd, $J_{C,F}$ = 7 Hz, $J_{C,F}$ = 8 Hz), 122.2, 122.4, 122.5, 123.6, 125.3,

125.85, 125.89, 125.93, 128.1 (m), 143.0, 143.2, 143.9, 144.3, 151.77 (dd, $^2J_{C,F}$ = 15 Hz, $^1J_{C,F}$ = 256 Hz), 151.79 (dd, $^2J_{C,F}$ = 15 Hz, $^1J_{C,F}$ = 256 Hz). ^{19}F NMR (376 MHz, $CDCl_3$): δ -259.90 - -259.89 (m, 2F). IR (KBr): 3068, 3017, 2958, 2896, 2179, 1607, 1554, 1501, 1473, 1457, 1324, 1290, 1249, 1230, 1214, 1190, 1092, 1070, 1052, 1032, 1026, 986, 942, 854, 843, 819, 750, 703, 676, 656, 639, 626, 607, 488 cm^{-1}. MS, *m/z* (%): 785.2 (100, M + Na). HRMS, (ESI+) for ($C_{55}H_{36}F_2{}^{28}Si$ + $^{23}Na^+$): calcd 785.2447, found 785.2448. Anal. Calcd. for $C_{55}H_{36}F_2Si$: C, 86.58; H, 4.76. Found: C, 86.41; H, 4.62.

Compound 18. A flame-dried Schlenk flask was charged with iodide **12** (300 mg, 0.622 mmol, 1.0 equiv.), alkyne **7** (303 mg, 0.809 mmol, 1.3 equiv.), $Pd(PPh_3)_4$ (29 mg, 0.025 mmol, 4 mol %), and CuI (4 mg, 0.019 mmol, 3 mol %). After three successive vacuum/argon cycles, degassed dry THF (10 mL) and triethylamine (10 mL) were added from a syringe. The slightly yellowish solution was stirred for 16 h at the temperature of the oil bath 55 °C. A dense white solid precipitated. The crude reaction mixture was cooled to room temperature, diluted with CH_2Cl_2 (100 mL) and washed with saturated aqueous NH_4Cl (2 × 20 mL). The clear yellowish organic phase was dried over $MgSO_4$ and volatiles were removed under reduced pressure. Column chromatography on silica gel (hexane/CH_2Cl_2 - 1:2 to elute impurities and then CH_2Cl_2 to elute product) gave **18** as a white crystalline solid (378 mg, 0.519 mmol, 83%).

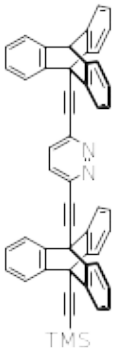

Mp > 300 °C (dec.). ^{1}H NMR (400 MHz, $CDCl_3$): δ 0.50 (s, 9H), 5.50 (s, 1H), 7.08 – 7.15 (m, 6H), 7.15 – 7.20 (m, 6H), 7.45 – 7.47 (m, 3H), 7.79 – 7.82 (m, 3H), 7.89 – 7.91 (m, 6H), 8.01 (br s, 2H). ^{13}C {^{1}H} NMR (100 MHz, $CDCl_3$): δ 0.3, 52.8, 53.1, 53.3, 53.6, 89.2, 89.5, 90.7, 91.2, 98.4, 99.2, 122.2, 122.4, 122.5, 123.6, 125.4, 125.9, 126.00, 126.03, 129.39, 129.42, 142.7, 143.2, 143.5, 144.3, 145.9, 146.1. IR (KBr): 3069, 3018, 2958, 2925, 2898, 2852, 2248, 2181, 1607, 1531, 1457, 1403, 1310, 1250, 1170, 1155, 1139, 1073, 1032, 909, 855, 846, 752, 729, 696, 640, 608, 486 cm^{-1}. MS, *m/z* (%): 729.3 (100, M + H). HRMS, (ESI+) for ($C_{53}H_{36}N_2Si$ + H^+): calcd 729.2721, found 729.2724. Anal. Calcd. for $C_{53}H_{36}N_2Si$: C, 87.33; H, 4.98; N, 3.84. Found: C, 87.11; H, 4.86; N, 3.80.

Compound 19. A flame-dried Schlenk flask was charged with iodide **16** (400 mg, 0.833 mmol, 1.0 equiv.), alkyne **7** (406 mg, 1.083 mmol, 1.3 equiv.), $Pd(PPh_3)_4$ (39 mg, 0.033 mmol, 4 mol %), and CuI (5 mg, 0.025 mmol, 3 mol %). After three successive vacuum/argon cycles, degassed dry THF (10 mL) and triethylamine (8 mL) were added from a syringe. The slightly yellowish solution was stirred for 16 h at the temperature of the oil bath 80 °C. A dense white solid precipitated. The crude reaction mixture was cooled to room temperature, diluted with CH_2Cl_2 (150 mL) and washed with saturated aqueous NH_4Cl (2 × 30 mL). The clear yellowish organic phase was dried over $MgSO_4$ and volatiles were removed under reduced pressure. Column chromatography on silica gel (hexane/CH_2Cl_2 - 4:1, then hexane/CH_2Cl_2 – 1:1) gave **19** as a white crystalline solid (514 mg, 0.707 mmol, 85%).

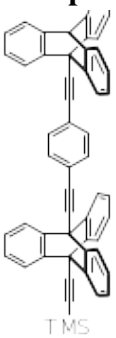

Mp > 300 °C (dec.). ^{1}H NMR (400 MHz, $CDCl_3$): δ 0.50 (s, 9H), 5.49 (s, 1H), 7.07 – 7.14 (m, 6H), 7.15 – 7.17 (m, 6H), 7.43 – 7.45 (m, 3H), 7.78 – 7.80 (m, 3H), 7.85 – 7.88 (m, 6H), 7.94 (s, 4H). ^{13}C {^{1}H} NMR (100 MHz, $CDCl_3$): δ 0.4, 52.9, 53.1, 53.3, 53.6, 85.5, 86.0, 92.2, 92.6, 98.2, 99.5, 122.2, 122.4, 122.5, 123.1, 123.4, 123.5, 125.2, 125.76, 125.78, 125.82, 132.2, 132.3, 143.3, 143.4, 144.3, 144.4. IR (KBr): 3068, 3035, 3017, 2957, 2897, 2233, 2180, 1607, 1508, 1453, 1404, 1312, 1289, 1250, 1190, 1154, 1137, 1101, 1071, 1044, 1032,

942, 876, 855, 836, 750, 720, 694, 633, 640, 608, 554, 547, 522, 485 cm^{-1}. MS, *m/z* (%): 727.3 (100, M + H). HRMS, (APCI) for ($C_{55}H_{38}Si + H^+$): calcd 727.2816, found 727.2812. Anal. Calcd. for $C_{55}H_{38}Si$: C, 90.87; H, 5.27. Found: C, 90.66; H, 5.40.

General procedure for TMS removal (GP 2). To a stirred solution of silyl derivatives **17**-**19** (1 equiv) in wet THF (8 mL), a solution of TBAF in THF (1.0 M, 1.2 equiv) was added at room temperature. The reddish reaction mixture was stirred for 30 min, diluted with CH_2Cl_2 (150 mL), washed with water (2 × 30 mL), and the clear yellowish organic phase was dried over $MgSO_4$. Solvents were removed under reduced pressure and a column chromatography on silica gel gave alkynes **20**-**22** as white crystalline solids.

Compound 20 was prepared from silyl derivative **17** (350 mg, 0.459 mmol, 1.0 equiv.), and a solution of TBAF in THF (1.0 M, 596 µL, 596 mmol, 1.3 equiv.) in THF (15 mL) according to **GP2**. Column chromatography on silica gel (hexane/CH_2Cl_2 – 2:1) gave alkyne **20** as a white crystalline solid (314 mg, 0.455 mmol, 99%).

Mp > 300 °C (dec.). ^{1}H NMR (400 MHz, $CDCl_3$): δ 3.35 (s, 1H), 5.50 (s, 1H), 7.08 – 7.16 (m, 6H), 7.17 – 7.20 (m, 6H), 7.45 – 7.47 (m, 3H), 7.66 (s, 1H), 7.67 (s, 1H), 7.83 – 7.89 (m, 9H). ^{13}C {^{1}H} NMR (100 MHz, $CDCl_3$): δ 52.3, 53.1, 53.3, 53.8, 77.9, 81.1, 84.5 (m), 84.9 (m), 92.0 (d, $J_{C,F}$ = 2 Hz), 92.7 (d, $J_{C,F}$ = 3 Hz), 114.0 (dd, $J_{C,F}$ = 4 Hz, $J_{C,F}$ = 11 Hz), 114.4 (dd, $J_{C,F}$ = 7 Hz, $J_{C,F}$ = 8 Hz), 122.2, 122.3, 122.4, 123.6, 125.3, 125.90, 125.95, 125.98, 128.1 (m), 143.0, 143.9, 144.3, 151.77 (dd, $^2J_{C,F}$ = 15 Hz, $^1J_{C,F}$ = 256 Hz), 151.80 (dd, $^2J_{C,F}$ = 15 Hz, $^1J_{C,F}$ = 256 Hz). ^{19}F NMR (376 MHz, $CDCl_3$): δ -256.89 - -256.88 (m, 2F). IR (KBr): 3304, 3068, 3018, 2960, 2246, 1623, 1608, 1582, 1558, 1500, 1473, 1457, 1324, 1290, 1232, 1213, 1190, 1160, 1087, 1069, 1040, 1033, 1026, 985, 942, 909, 868, 820, 751, 695, 680, 658, 640, 626, 607, 529, 487 cm^{-1}. MS, *m/z* (%): 713.2 (100, M + Na). HRMS, (ESI+) for ($C_{52}H_{28}F_2 + {}^{23}Na^+$): calcd 713.2051, found 713.2049. Anal. Calcd. for $C_{52}H_{28}F_2 + CDCl_3$ in 3:1 ratio: C, 86.00; H, 3.95. Found: C, 85.66; H, 3.94.

Compound 21 was prepared from silyl derivative **18** (320 mg, 0.487 mmol, 1.0 equiv.), and a solution of TBAF in THF (1.0 M, 633 µL, 633 mmol, 1.3 equiv.) in THF (15 mL) according to **GP2**. Column chromatography on silica gel (CH_2Cl_2) gave alkyne **21** as white crystalline solid (290 mg, 0.442 mmol, 91%).

Mp > 300 °C (dec.). ^{1}H NMR (400 MHz, $CDCl_3$): δ 3.35 (s, 1H), 5.49 (s, 1H), 7.07 – 7.15 (m, 6H), 7.15 – 7.20 (m, 6H), 7.44 – 7.46 (m, 3H), 7.82 – 7.84 (m, 3H), 7.87 – 7.91 (m, 6H), 8.01 (br s, 2H). ^{13}C {^{1}H} NMR (100 MHz, $CDCl_3$): δ 52.3, 52.9, 53.3, 53.6, 77.8, 81.1, 89.1, 89.5, 90.5, 91.3, 122.3, 122.4, 123.7, 125.4, 125.98, 126.00, 126.1, 129.39, 129.43, 142.6, 142.9, 143.5, 144.3, 145.9, 146.1. IR (KBr): 3295, 3068, 3017, 2960, 2921, 2850, 2246, 1608, 1526, 1457, 1404, 1310, 1290, 1281, 1265, 1236, 1170, 1155, 1032, 976, 946, 911, 877, 846, 751, 673, 660, 640, 607, 569, 485 cm^{-1}. MS, *m/z* (%): 657.2 (100, M + H). HRMS, (APCI) for ($C_{50}H_{28}N_2 + H^+$): calcd 657.2325, found 657.2326. Anal. Calcd. for $C_{50}H_{28}N_2 + CH_2Cl_2$ in 3:4 ratio: C, 80.07; H, 4.01; N, 3.64. Found: C, 79.89; H, 4.14; N, 3.49.

Compound 22 was prepared from silyl derivative **19** (450 mg, 0.619 mmol, 1.0 equiv.), and a solution of TBAF in THF (1.0 M, 805 µL, 0.805 mmol, 1.3 equiv.) in THF (15 mL)

according to **GP2**. Column chromatography on silica gel (hexane/CH_2Cl_2 – 2:1) gave alkyne **19** as a white poorly soluble crystalline solid (398 mg, 0.608 mmol, 98%).

Mp > 300 °C (dec.). ^{1}H NMR (400 MHz, THF-d_8): δ 3.97 (s, 1H), 5.56 (s, 1H), 7.01 – 7.08 (m, 6H), 7.10 – 7.16 (m, 6H), 7.42 – 7.44 (m, 3H), 7.77 – 7.79 (m, 3H), 7.80 – 7.83 (m, 3H), 7.85 – 7.87 (m, 3H), 8.02 (s, 4H). ^{13}C {^{1}H} NMR (100 MHz, THF-d_8): δ 53.4, 54.0, 54.2, 54.7, 78.7, 83.2, 86.3, 87.1, 93.3, 93.8, 123.06, 123.13, 124.1, 124.4, 124.6, 125.9, 126.5, 126.67, 126.70, 133.3, 144.4, 144.6, 145.5, 145.9. IR (KBr): 3308, 3068, 3015, 2953, 2240, 1607, 1508, 1453, 1405, 1314, 1289, 1233, 1189, 1178, 1169, 1154, 1101, 1067, 1032, 1027, 943, 876, 837, 749, 687, 659, 651, 640, 607, 545, 523, 496, 491, 483 cm^{-1}. MS, *m/z* (%): 655.2 (100, M + H). HRMS, (APCI) for ($C_{52}H_{30}$ + H^+): calcd 655.2420, found 655.2421. Anal. Calcd. for $C_{52}H_{30}$ + THF in 3:2 ratio: C, 93.42; H, 5.07. Found: C, 93.64; H, 5.02.

General procedure for carboxylation (GP 3). A solution of LiHMDS in THF (1.0 M, 1.5 equiv.) was added dropwise to a stirred solution of **20**, **21**, and **22** (1.0 equiv.) in THF (15 - 60 mL) at -78 °C. It was stirred for 10 min at -78 °C, $ClCOOCH_3$ (2.0 equiv.) was added, and the resulting slightly yellowish solution was stirred for 15 min at -78 °C. Cooling was discontinued, the reaction mixture was slowly warmed to room temperature and stirred for additional 60 min. It was diluted with ether (150 mL), washed with saturated aqueous NH_4Cl (2 × 25 mL), and the clear yellowish organic phase was dried over $MgSO_4$. Volatiles were removed under reduced pressure. Column chromatography on silica gel provided the esters **23**, **24**, and **25** as white crystalline solids.

Compound 23 was prepared from alkyne **20** (300 mg, 0.434 mmol, 1.0 equiv.), LiHMDS in THF (1.0 M, 651 µL, 0.651 mmol, 1.5 equiv.), and $ClCOOCH_3$ (67 µL, 0.868 mmol, 2.0 equiv.) in THF (15 mL) according to **GP3**. Column chromatography on silica gel (hexane/CH_2Cl_2 - 1:1) gave ester **23** as a white crystalline solid (314 mg, 0.419 mmol, 97%).

Mp > 300 °C (dec.). ^{1}H NMR (400 MHz, $CDCl_3$): δ 4.02 (s, 3H), 5.50 (s, 1H), 7.08 – 7.16 (m, 6H), 7.19 – 7.22 (m, 6H), 7.45 – 7.47 (m, 3H), 7.67 – 7.68 (m, 2H), 7.78 – 7.80 (m, 3H), 7.85 – 7.90 (m, 6H). ^{13}C {^{1}H} NMR (100 MHz, $CDCl_3$): δ 52.1, 53.1, 53.2, 53.3, 53.8, 81.9, 84.2, 84.4 (d, $J_{C,F}$ = 4 Hz), 85.1 (d, $J_{C,F}$ = 4 Hz), 91.6 (d, $J_{C,F}$ = 3 Hz), 92.8 (d, $J_{C,F}$ = 3 Hz), 113.8 (dd, $J_{C,F}$ = 2 Hz, $J_{C,F}$ = 12 Hz), 114.5 (dd, $J_{C,F}$ = 4 Hz, $J_{C,F}$ = 11 Hz), 122.2, 122.4, 122.5, 123.6, 125.3, 125.9, 126.2, 126.3, 128.0 (d, $J_{C,F}$ = 4 Hz), 128.1 (d, $J_{C,F}$ = 4 Hz), 142.0, 142.7, 143.9, 144.3, 151.76 (dd, $^2J_{C,F}$ = 15 Hz, $^1J_{C,F}$ = 256 Hz), 151.80 (dd, $^2J_{C,F}$ = 15 Hz, $^1J_{C,F}$ = 256 Hz), 153.8. ^{19}F NMR (376 MHz, $CDCl_3$): δ -256.85 - -256.81 (m, 2F). IR (KBr): 3068, 3036, 3017, 2953, 2247, 1719, 1622, 1607, 1554, 1500, 1472, 1457, 1435, 1322, 1306, 1290, 1266, 1231, 1211, 1191, 1166, 1096, 1071, 1059, 1033, 1026, 986, 942, 909, 868, 820, 750, 733, 698, 683, 650, 607, 487 cm^{-1}. MS, *m/z* (%): 771.2 (100, M + Na). HRMS, (ESI+) for ($C_{54}H_{30}F_2O_2$ + $^{23}Na^+$): calcd 771.2106, found 771.2109. Anal. Calcd. for $C_{54}H_{30}F_2O_2$ + $CDCl_3$ in 5:3 ratio: C, 79.87; H, 3.83. Found: C, 79.89; H, 3.74.

Compound 24 was prepared from alkyne **21** (250 mg, 0.381 mmol, 1.0 equiv.), LiHMDS in THF (1.0 M, 572 µL, 0.572 mmol, 1.5 equiv.), and $ClCOOCH_3$ (59 µL, 0.762 mmol, 2.0 equiv.) in THF (30 mL) according to **GP3**. Column chromatography on silica gel (CH_2Cl_2) gave ester **24** as a white crystalline solid (165 mg, 0.231 mmol, 61%).

Mp > 300 °C (dec.). ^{1}H NMR (400 MHz, $CDCl_3$): δ 4.01 (s, 3H), 5.50 (s, 1H), 7.08 – 7.15 (m, 6H), 7.17 – 7.22 (m, 6H), 7.45 – 7.47 (m, 3H), 7.77 – 7.79 (m, 3H), 7.88 – 7.93 (m, 6H), 8.00 (br s, 2H). ^{13}C {^{1}H} NMR (100 MHz, $CDCl_3$): δ 52.2, 52.9, 53.2, 53.3, 53.6, 81.7, 84.3, 89.1, 89.7, 90.0, 91.3, 122.3, 122.4, 122.5, 123.7, 125.4, 126.0, 126.25, 126.30, 129.3, 129.4, 142.0, 142.4, 143.5, 144.3, 145.8, 146.2, 153.8. IR (KBr): 3068, 3017, 2954, 2245, 1718, 1607, 1528, 1455, 1435, 1398, 1314, 1289, 1263, 1226, 1083, 1032, 1027, 975, 945, 914, 861, 846, 749, 677, 662, 639, 607, 480 cm^{-1}. MS, *m/z* (%): 737.6 (25, M + Na), 715.6 (100, M + H). HRMS, (ESI+) for ($C_{52}H_{30}N_2O_2$ + H^+): calcd 715.2380, found 715.2376. Anal. Calcd. for $C_{52}H_{30}N_2O_2$: C, 87.37; H, 4.23; N, 3.92. Found: C, 87.56; H, 4.21; N, 3.68.

Compound 25 was prepared from alkyne **22** (350 mg, 0.535 mmol, 1.0 equiv.), LiHMDS in THF (1.0 M, 802 µL, 0.802 mmol, 1.5 equiv.), and $ClCOOCH_3$ (83 µL, 1.070 mmol, 2.0 equiv.) in THF (60 mL) according to **GP3**. Column chromatography on silica gel (hexane/CH_2Cl_2 - 1:1) gave ester **25** as a white crystalline solid (335 mg, 0.470 mmol, 88%).

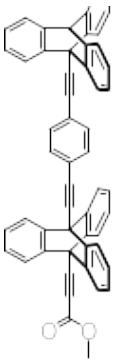

Mp > 300 °C (dec.). ^{1}H NMR (400 MHz, $CDCl_3$): δ 4.02 (s, 3H), 5.49 (s, 1H), 7.07 – 7.14 (m, 6H), 7.17 – 7.20 (m, 6H), 7.43 – 7.45 (m, 3H), 7.76 – 7.78 (m, 3H), 7.84 – 7.86 (m, 3H), 7.87 – 7.89 (m, 3H), 7.94 (s, 4H). ^{13}C {^{1}H} NMR (100 MHz, $CDCl_3$): δ 52.1, 53.0, 53.2, 53.3, 53.6, 82.0, 84.2, 85.0, 86.1, 92.2, 92.8, 122.1, 122.5, 122.6, 122.9, 123.52, 123.54, 125.2, 125.8, 126.0, 126.2, 132.26, 132.30, 142.1, 143.2, 144.3, 144.4, 153.9. IR (KBr): 3067, 3037, 3017, 2952, 2247, 1723, 1607, 1508, 1454, 1432, 1404, 1318, 1298, 1264, 1224, 1183, 1169, 1101, 1084, 1045, 1032, 1026, 1018, 974, 945, 876, 862, 836, 749, 675, 656, 649, 640, 607, 545, 522, 485 cm^{-1}. MS, *m/z* (%): 713.2 (100, M + H), 655.2 (68, M – $COOCH_3$). HRMS, (APCI) for ($C_{54}H_{32}O_2$ + H^+): calcd 713.2475, found 713.2476. Anal. Calcd. for $C_{54}H_{32}O_2$: C, 90.99; H, 4.52. Found: C, 90.75; H, 4.72.

ASSOCIATED CONTENT

Supporting Information. The Supporting Information is available free of charge on the ACS Publications website.

Parameters of single crystals, Langmuir-Blodgett isotherms for **1**-**3**, comparison of infrared spectra of **1**-**3** in KBr and corresponding 2-D films, copies of ^{1}H and ^{13}C NMR spectra of all new compounds, and an ORTEP view of a single molecule and packing in **1**, **2**, **11**, **13** and **16** (PDF).

X-ray crystallographic data for compound **1** (CIF)
X-ray crystallographic data for compound **2** (CIF)
X-ray crystallographic data for compound **11** (CIF)
X-ray crystallographic data for compound **13** (CIF)
X-ray crystallographic data for compound **16** (CIF)

Accession Codes

CCDC xyz-xyz contain the supplementary crystallographic data for this paper. These data can be obtained free of charge via www.ccdc.cam.ac.uk/data_request/cif, or by emailing data_request@ccdc.cam.ac.uk, or by contacting The Cambridge Crystallographic Data Centre, 12 Union Road, Cambridge CB2 1EZ, UK; fax: +44 1223 336033.

AUTHOR INFORMATION

Corresponding Author

* kaleta@uochb.cas.cz

ORCID
I. Císařová: 0000-0002-9612-9831
J. Kaleta: 0000-0002-5561-7580

Notes
The authors declare no competing financial interest.

ACKNOWLEDGEMENTS

This work was supported by the Institute of Organic Chemistry and Biochemistry of the Czech Academy of Sciences (RVO: 61388963), Czech Science Foundation (grant number: 20-13745S). We thank Dr. Lucie Bednárová for help with IR spectra and Dr. Veronika Šolínová and Dr. Václav Kašička for determining the acidity constants. The Advanced Light Source is supported by the Director, Office of Science, Office of Basic Energy Sciences, of the U.S. Department of Energy under Contract No. DE-AC02-05CH11231.

REFERENCES

[1] . García-López, V.; Liu, D.; Tour, J. M. "Light-Activated Organic Molecular Motors and Their Applications" *Chem. Rev.* **2020**, *120*, 79–124.

[2] . Baroncini, M.; Silvi, S.; Credi, A. "Photo- and Redox-Driven Artificial Molecular Motors" *Chem. Rev.* **2020**, *120*, 200–268.

[3] . Corra, S.; Curcio, M.; Baroncini, M.; Silvi, S.; Credi, A. "Photoactivated Artificial Molecular Machines that Can Perform Tasks" *Adv. Mater.* **2020**, *32*, 1906064.

[4] . Casalini, S.; Bortolotti, C. A.; Leonardi, F.; Biscarini, F. "Self-Assembled Monolayers in Organic Electronics" *Chem. Soc. Rev.* **2017**, *46*, 40-71.

[5] . Klajn, R. "Immobilized Azobenzenes for the Construction of Photoresponsive Materials" *Pure Appl. Chem.* **2010**, *82*, 2247-2279.

[6] . Ichimura, K.; Oh, S. K.; Nakagawa, M. "Light-Driven Motion of Liquids on a Photoresponsive Surface" *Science*, **2000**, *288*, 1624-1626.

[7] . Perego, J.; Bracco, S.; Negroni, M.; Bezuidenhout, C. X.; Prando, G.; Carretta, P.; Comotti, A.; Sozzani, P. "Fast Motion of Molecular Rotors in Metal-Organic Framework Struts at Very Low Temperatures" *Nat. Chem.* **2020**, *12*, 845-851.

[8] . Zhao, K.; Dron, P. I.; Kaleta, J.; Rogers, C. T.; Michl, J. "Arrays of Dipolar Molecular Rotors in Tris(*o*-phenylenedioxy)cyclotriphosphazene" *Top. Curr. Chem.* **2014**, *354*¸ 163-212.

[9] . Liepuoniute, I.; Jellen, M. J.; Garcia-Garibay, M. A. "Correlated Motion and Mechanical Gearing in Amphidynamic Crystalline Molecular Machines" *Chem. Sci. 11*, 12994–13007.

[10] . Lemouchi, C.; Iliopoulos, K.; Zorina, L.; Simonov, S.; Wzietek, P.; Cauchy, T.; Fortea, A.; Canadell, E.; Kaleta, J.; Michl, J.; Gindre, D.; Chrysos, M.; Batail, P. "Crystalline Arrays of Pairs of Molecular Rotors: Correlated Motion, Rotational Barriers, and Space-Inversion Symmetry Breaking Due to Conformational Mutations" *J. Am. Chem. Soc.* **2013**, *135*, 9366-9376.

[11] . Wagner, S.; Leyssner, F.; Kördel, C.; Zarwell, S.; Schmidt, R.; Weinelt, M.; Rück-Braun, K.; Wolf, M.; Tegeder, P. "Reversible Photosiomerization of an Azobenzene-Functionalized Self-Assembled Monolayer Probed by Sum-Frequency Generation Vibrational Spectroscopy" *Phys. Chem. chem. Phys.* **2009**, *11*, 6242-6248.

[12] . Chen, K.-Y.; Ivashenko, O.; Caroll, G. T.; Robertus, J.; Kistemaker, J. C. M.; London, G.; Browne, W. R.; Rudolf, P.; Feringa, B. L. "Control of Surface Wettability Using Tripodal Light-Activated Molecular Motors" *J. Am. Chem. Soc.* **2014**, *136*, 3219-3224.

[13] . Krajnik, B.; Chen, J.; Watson, M. A.; Cockroft, S. L.; Feringa, B. L.; Hotkens, J. "Defocused Imaging of UV-Driven Surface-Bound Molecular Motors" *J. Am. Chem. Soc.* **2017**, *139*, 7156-7159.

[14] . Kaleta, J.; Kaletová, E.; Císařová, I.; Teat, S. J.; Michl, J. "Synthesis of Triptycene-Based Molecular Rotors for Langmuir-Blodgett Monolayers" *J. Org. Chem.* **2015**, *80*, 10134-10150.

[15] . Kaleta, J.; Wen, J.; Magnera, T. F.; Dron, P. I.; Zhu, C.; Michl, J. "Structure of a Monolayer of Molecular Rotors on Aqueous Subphase from Grazing-Incidence X-Ray Diffraction" *PNAS* **2018**, *115*, 9373-9378.

[16] . Kaleta, J.; Chen, J.; Bastien, G.; Dračínský, M.; Mašát, M.; Rogers, C. T.; Feringa, B. L.; Michl, J. "Surface Inclusion of Unidirectional Molecular Motors in Hexagonal Tris-(*o*-phenylenedioxy)cyclotriphosphazene TPP" *J. Am. Chem. Soc.* **2017**, *139*, 10486-10498.

[17] . Santos Hurtado, C.; Bastien, G.; Mašát, M.; Štoček, J. R.; Dračínský, M.; Rončević, I.; Císařová, I.; Rogers, C. T.; Kaleta, J. "Regular 2-D Arrays of Surface-Mounted Molecular Switches: Switching Monitored by UV-vis and NMR Spectroscopy" *J. Am. Chem. Soc.* **2020**, *142*, 9337-9351.

[18] . Kaleta, J.; Dron, P. I.; Zhao, K.; Shen, Y.; Císařová, I.; Rogers, C. T.; Michl, J. "Arrays of Molecular Rotors with Triptycene Stoppers: Surface Inclusion in Hexagonal Tris(*o*-phenylenedioxy)cyclotriphosphazene" *J. Org. Chem.* **2015**, *80*, 6173-6192.

[19] . Baisch, B.; Raffa, D.; Jung, U.; Magnussen, O. M.; Nicolas, C.; Lacour, J.; Kubitschke, J.; Herges, R. "Mounting Freestanding Molecular Functions onto Surfaces: The Platform Approach" *J. Am. Chem. Soc.* **2009**, *131*, 442-443.

[20] . Ishiwari, F.; Nascimbeni, G.; Sauter, E.; Tago, H.; Shoji, Y.; Fujii, S.; Kiguchi, M.; Tada, T.; Zharnikov, M.; Zojer, E.; Fukushima, T. "Triptycene Tripods for the Formation of Highly Uniform and Densely Packed Self-Assembled Monolayers with Controlled Molecular Orientation" *J. Am. Chem. Soc.* **2019**, *141*, 5995–6005.

[21] . Nygaard, L.; Hansen, R. E.; Hansen, L. R.; Andersen, J. R.; Sorensen, G. O. "Microwave Spectra and Dipole Moments of 1,2-Difluorobenzene and 1,3-Difluorobenzene" *Spectrochimica Acta* **1967**, *23A*, 2813-2819.

[22] . Li, H.; Franks, K. J.; Hanson, R. J.; Kong, W. "Brute Force Orientation and Alignment of Pyridazine Probed by Resonantly Enhanced Multiphoton Ionization" *J. Phys. Chem. A* **1998**, *102*, 8084.

[23] . Letsinger, R.; Lasco, R. "Reactions of Organometallics Compounds with Pyridazine" *J. Org. Chem.* **1956**, *21*, 812-814.

[24] . Riwar, L.-J.; Trapp, N.; Kuhn, B.; Diederich, F. "Substituent Effects in Parallel-Displaced π–π Stacking Interactions: Distance Matters" *Angew. Chem., Int. Ed.* **2017**, *56*, 11252-11257.

[25] . Murray, B. S.; Grieser, F.; Healy, T. W.; Scales, P. J. "Spectroscopic and Electrokinetic Study of the pH-Dependent Ionization of Langmuir-Blodgett Films" *Langmuir* **1992**, *8*, 217-221.

[26] . Chaiko, D. J.; Osseo-Asare, K. "Behavior of Dinonylnaphthalene Sulfonate Monolayers at the Air–Water Interface" *Colloids and Surfaces A: Physicochemical and Engineering Aspects* **2000**, *175*, 335-347.

[27] . Šolínová, V.; Kašička, V. "Determination of Acidity Constants and Ionic Mobilities of Polyprotic Peptide Hormones by Capillary Zone Electrophoresis" *Electrophoresis* **2013**, *34*, 2655-2665.

[28] . Kaleta, J.; Bednárová, L.; Čížková, M.; Wen, J.; Kaletová, E.; Michl, J. "IR Spectra of *n*-Bu_4M (M = Si, Ge, Sn, Pb), *n*-$BuAuPPh_3$-d_{15}, and of "*n*-Bu" on a Gold Surface." *J. Phys. Chem. A* **2017**, *121*, 4619-4625.

[29] . Sheldrick, G. M. "Crystal structure refinement with SHELXL" *Acta Cryst.* **2008**, *A64*, 112.

[30] . Rausis, T.; Schlosser, M. "The Basicity Gradient-Driven Migration of Iodine: Conferring Regioflexibility on the Substitution of Fluoroarenes" *Eur. J. Org. Chem.* **2002**, 3351-3358.